7. Induction Machine Based Drive Systems

In most cases, industrial drive systems are based on induction machines. They are used as line-fed **"constant speed"** drives, where the speed is very close to synchronous speed, hence, it is almost constant, as well as inverter-fed **variable speed** drives.

7.1 Typical Work Machines

Drive systems drive different **loads**, that can be characterised by their **torque-speed characteristic** $M_s(n)$. Four different types are distinguished (Fig. 7.2a).

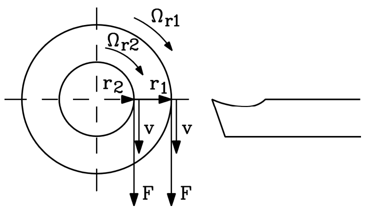

a)


b)

Fig 7.1: Examples of work machines: a) **constant power load**: Cutting force F and cutting speed v shall be constant to assure optimum cutting. Therefore, the cutting power $P = F v$ has to be constant, independently of the speed. b) variable speed **drives for pump drives** in a groundwater pumping station

1) Constant Torque:
The load torque of **lifting machines** (**elevators, cranes**, ...) is constant, independently of the motor speed. It is – e.g. in the case of a conveyer cabin (mass m) at a rope drum (diameter d) – determined by the acceleration of gravity $g = 9.81$ m/s^2 (7.1).

$$M_s = m \cdot g \cdot (d/2) \quad \Rightarrow \quad M_s = const. \tag{7.1}$$

Piston compressors, e.g. for air compression (generation of compressed air), also have a constant torque.

2) Torque Increases Linear with the Speed:
The torque of **extruders** and similar machines used for manufacturing and processing of **plastics** increases linear with the speed.

$$M_s \sim n \tag{7.2}$$

3) Torque Increases with the Square of the Speed:
Rotating machines for fluids (pumps, fans, ventilators, turbo compressors, propellers, etc.) obey to *EULER*'s fundamental law of turbines (Chapter 5). Their torque increases with the square of the speed (Fig. 7.1b).

$$M_s \sim n^2 \tag{7.3}$$

4) Torque Decreases Inversely Proportional with the Speed ("Constant Power Drives"):
Cutting and milling in tooling machines, winder machines as well as **rolling drives** operate with constant speed v and force F (Fig 7.1a). As the radius r e.g. of the working piece during cutting (Fig. 7.2a) decreases during the operation, the speed $n = v/(2\pi r)$ has to increase to maintain v constant. At the same time, the torque $M_s = F r$ decreases, because F is constant. The mechanical power $P = 2\pi n M_s = F v$ remains constant (**"constant power drives"**), and the torque decreases inversely proportional to the speed.

$$v = \Omega_{r1} \cdot r_1 = \Omega_{r2} \cdot r_2 = const. \quad \Leftrightarrow \quad \Omega_r = 2\pi \cdot n \quad \Rightarrow \quad n = \frac{v}{2\pi \cdot r} \tag{7.4a}$$

$$M_s = P/(2\pi \cdot n) \sim 1/n \tag{7.4b}$$

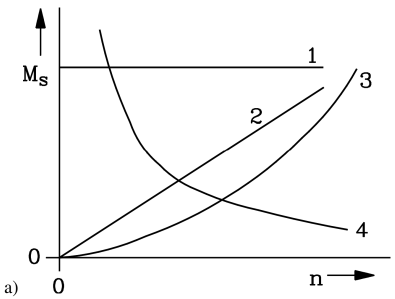

a)


b)


c)

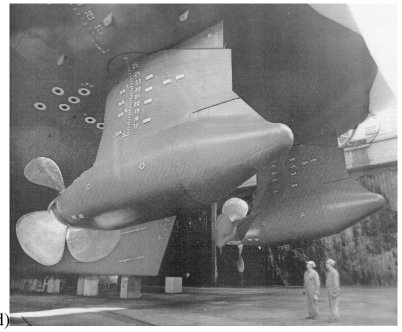
d)

Fig 7.2: Work machines: a) torque characteristics, 1: lifting machines, 2: extruders, 3: rotating fluid machines, 4: constant power drives, b) electric car (DaimlerChrysler), c) induction motor driven high-speed train ICE3, d) synchronous motor driven ship propulsion

Drives of **electric trains** or **cars** have similar characteristics. At low speed, a high torque is required to allow for quick start-up or acceleration of a heavy goods train at a ramp. At high speed, a small torque is sufficient, because only friction and wind forces and gravity on slopes have to be overcome. Here, with high speed trains (e.g. ICE3: $v_{max} = 330$ km/h), the wind force is the dominating braking factor. Therefore, the torque demand decreases as the speed increases.

7.2 Running Up of Line-Fed Induction Machines

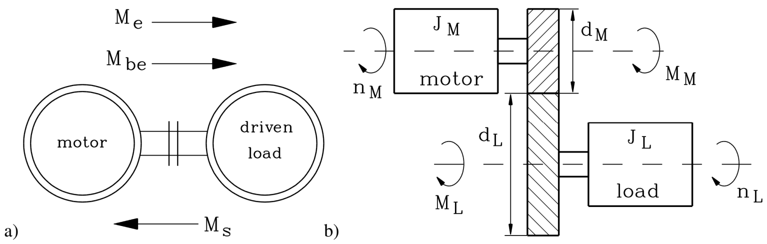

Fig. 7.3: Coupling of motor and load, a) directly coupled drive ($n_M = n_L = n$), b) drive with gear (transfer ratio $i = n_M/n_L$)

a) Dynamic Equations:
An induction motor (**polar moment of inertia** of the rotor J_M, subscript M: motor), which is directly coupled with a load (polar moment of inertia J_L, subscript L: load), is considered (Fig. 7.3a). The induction motor drives the load at the shaft. At the shaft, the electromagnetic torque M_e generated in the air gap of the machine minus the motor loss torque M_d (friction) and the braking (negative) torque of the load M_s are effective. *NEWTONS*'s first law (**equation for mechanical movement**) is applied to calculate the angular acceleration $d\Omega_m / dt$ of the coupled machines. The sum of the positive and negative torque gives the accelerating torque M_{be}, which equals the change of the angular momentum (angular momentum: $(J_{L+M} \cdot \Omega_m)$).

$$(J_L + J_M)\frac{d\Omega_m}{dt} = M_e - M_d - M_s \quad \Rightarrow \quad \boxed{J_{L+M} \cdot \frac{d(2\pi n)}{dt} = M_{be}} \qquad (7.5)$$

If the motor and the load are coupled via a **gear** with the transfer ratio (Fig 7.3b)

$$i = n_M / n_L \ , \qquad (7.6)$$

load and motor turn at different speed. In the case of a simple **one stage gear unit** (Fig. 7.3b) this is realised by two interlocking gear wheels with diameters d_M and d_L that must have the same circumferential speed v and tangential force F at the point of contact.

$$v = d_M \pi n_M = d_L \pi n_L \quad \Rightarrow \quad i = n_M / n_L = d_L / d_M \qquad (7.7a)$$
$$F = 2M_M / d_M = 2M_s / d_L \quad \Rightarrow \quad i = M_s / M_M \quad M_M = M_s / i \qquad (7.7b)$$

The torque of the load M_s, but also the dynamic torque, which is given by the moment of inertia, is converted via i to the torque M_M that is effective at the motor shaft.

$$M_M = \frac{1}{i} \cdot \left(J_L \cdot d(2\pi n_L)/dt + M_s \right) \qquad (7.8)$$

During acceleration, the overall torque at the motor shaft is given by

$$J_M \frac{d2\pi n_M}{dt} = M_e - M_d - \frac{M_s}{i} - \frac{J_L}{i}\frac{d(2\pi n_L)}{dt} \quad \Rightarrow$$

$$\left(J_M + \frac{J_L}{i^2} \right) \cdot \frac{d(2\pi n_M)}{dt} = M_e - M_d - \frac{M_s}{i} . \qquad (7.9)$$

Result:
A gear transforms the moment of inertia of the load to the motor side by: $J = J_M + \frac{J_L}{i^2}$.

Example 7.1-1:
Gear of a high speed train: i = 2.5. The moment of inertia J_L of the slowly rotating wheel set ($n_{L,max}$ = 2200/min at 330 km/h) is effective on the motor side by $1/2.5^2$. How big is the maximum rotational speed of the motor? n_{max} = 2200·2.5 = 5500/min. How large is the diameter d of the driving wheels of the wheel set ? $d = v_{max}/(\pi \cdot n_{L,max})$ = 795 mm

In the following, the motor loss torque M_d due to the friction and windage losses P_R is neglected, hence, the shaft torque equals the air gap torque M_e.

b) Rated Acceleration Time:
The so-called **nominal acceleration time** (**starting time, run-up period**) $\boldsymbol{T_J}$ is the time that an uncoupled induction machine ("no-load": $M_s = 0, J_L = 0$), operating at its rated torque $M_e = M_N$, would take to accelerate from stand-still to rated speed:

$$J_M \frac{d\Omega_m}{dt} = M_N \quad \Rightarrow \quad \int_0^{\Omega_{mN}} d\Omega_m = \int_0^{T_J} \frac{M_N}{J_M} dt \quad \Rightarrow \quad \boxed{T_J = \frac{J_M}{M_N} \Omega_{mN}} \qquad (7.10)$$

With the rotor diameter d_r and the rotor stack length l, the moment of inertia of the rotor is $J_M \sim d_r^4 l$, whereas the torque is $M_e \sim d_r^2 l$ (see Chapter 8.1). Therefore, it is

$$T_J \sim d_r^2 . \qquad (7.11)$$

Result:
The nominal acceleration time of small machines is very small. It is below one second. Large machines may have a nominal acceleration time of 10 s and more. The nominal acceleration time is a "theoretical" value and characterises the size of the polar moment of inertia of the machine.

c) Acceleration Time and Energy Dissipated in the Rotor:
The **acceleration time** t_a is obtained by numerical integration of the differential equation (7.5), respectively (7.9) ($J = J_L + J_M$).

$$J \frac{d(2\pi n)}{dt} = M_e(n) - M_s(n) \quad \Rightarrow \quad \boxed{t_a = \int_0^{n_N} \frac{2\pi \cdot J}{M_e(n) - M_s(n)} \cdot dn} \qquad (7.12)$$

For a rough estimate of t_a, the average values $M_{e,av}$ and $M_{s,av}$ (average over the speed range 0...n_N) may be used (Fig. 7.4).

$$t_a \approx \int_0^{n_N} \frac{2\pi \cdot J}{M_{e,av} - M_{s,av}} \cdot dn \quad \Rightarrow \quad \boxed{t_a \approx \frac{2\pi n_N J}{M_{e,av} - M_{s,av}}} \qquad (7.13)$$

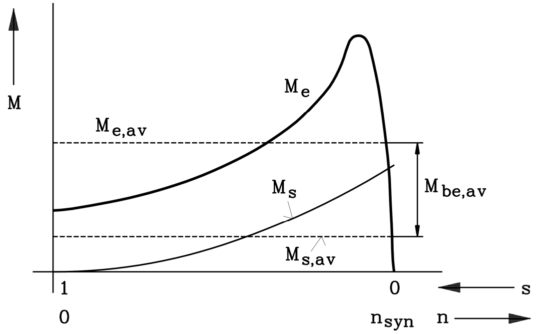

Fig 7.4: Torque-speed characteristic of an “induction motor compressor drive”. The average torque (subscript "av") is used for an approximate determination of the acceleration time.

A motor at no-load ($M_s = 0$) only has to accelerate the moment of inertia J (**“no load starting”**, **“centrifugal load starting”**). The energy $W_{Cu,r}$ that is dissipated in the rotor during the time t_a while the motor accelerates from 0 to $n_N \sim n_{syn}$ can be calculated exactly, independently of the torque-speed characteristic $M_e(n)$, because it is always $P_{Cu,r} = s \cdot P_\delta$ and $\Omega_m = (1-s)\Omega_{syn}$. The time range 0 ... t_a corresponds to the slip range 1 ... 0.

$$W_{Cu,r} = \int_0^{t_a} P_{Cu,r} \cdot dt = \int_0^{t_a} sP_\delta \cdot dt = \int_0^{t_a} s\Omega_{syn} M_e \cdot dt = \int_0^{t_a} s\Omega_{syn} J \frac{d\Omega_m}{dt} \cdot dt = \int_0^{t_a} s\Omega_{syn}^2 J \frac{d(1-s)}{dt} \cdot dt =$$

$$= -\int_0^{t_a} s\Omega_{syn}^2 J \frac{ds}{dt} dt = -\int_1^0 s\Omega_{syn}^2 J \cdot ds = -J\Omega_{syn}^2 \left. \frac{s^2}{2} \right|_1^0 = \frac{J\Omega_{syn}^2}{2} = W_{kin}$$

$$\boxed{W_{Cu,r} = W_{kin}} \qquad (7.14)$$

Result:
The copper losses which are dissipated in the rotor winding during no-load starting $W_{Cu,r}$ equal the kinetic energy W_{kin} that is stored in the rotating masses. If all other losses are neglected, the supplying grid has to supply the energy $2W_{kin}$ to allow for the running up. Half of this energy is converted into heat in the rotor winding, and the other half is stored in the rotating masses.

In the case of starting with a load torque M_s, the running up time is larger by the factor $M_{e,av} / (M_{e,av} - M_{s,av})$, according to (7.13). Hence, the dissipated energy increases by this factor.

$$W_{Cu,r} = \frac{J\Omega_{syn}^2}{2} \cdot \frac{M_{e,av}}{M_{e,av} - M_{s,av}} > W_{kin} \qquad (7.15)$$

<u>Example 7.2-1:</u>
Asynchronous running up of an induction motor with a double squirrel cage rotor:
P_N = 155 kW, f_N = 50 Hz, n_N = 974/min, J_M = 5.8 kgm^2, average asynchronous torque $M_{e;av}/M_N = 1.4$.
The directly coupled load has a much larger moment of inertia of J_L = 23.0 kgm^2 and an average load torque of $M_{s,av}/M_N = 0.7$.

(1) How big is the **pole count** of the motor, and how big is the **rated slip**?
As the rated speed is close to synchronous speed, the latter can only be 1000/min (at 50 Hz). Therefore, the motor **has six poles**.

$$n_{syn} = \frac{f_N}{p} = \frac{50}{3} = 16.66/s = 1000/min \Rightarrow 2p = \underline{\underline{6}}, \quad s_N = \frac{n_{syn} - n_N}{n_{syn}} = \frac{1000 - 974}{1000} = \underline{\underline{2.6\%}}$$

(2) What is the average **acceleration time** t_a up to rated speed?

$$J = 5.8 + 23.0 = 28.8 kgm^2, \quad M_N = \frac{P_N}{2\pi n_N} = \frac{155000}{2\pi \cdot (974/60)} = 1520 Nm$$

$$t_a = \frac{2\pi n_N J}{M_{e,av} - M_{s,av}} = \frac{2\pi \cdot (974/60) \cdot 28.8}{(1.4 - 0.7) \cdot 1520} = \underline{\underline{2.76 s}}$$

(3) **No-load running up** to synchronous speed (load machine coupled, load torque is zero): How much energy is dissipated in the rotor cage during running up?

$$W_{Cu,r} = \frac{28.8 \cdot (2\pi \cdot 1000/60)^2}{2} = \underline{\underline{158 kWs}}$$

(4) **Running up under load** up to rated speed: How much energy is dissipated in the rotor during running up?

$$W_{Cu,r} = \frac{28.8 \cdot (2\pi \cdot 974/60)^2}{2} \cdot \frac{1.4}{0.7} = \underline{\underline{300 kWs}}$$

d) Reduction of the Starting Current:
<u>d1) Star-Delta-Starting:</u>
The relatively high starting current of an induction machine (4 to 7 times the rated current) puts a strain on the grid and may lead to **voltage “sags”** during running up, notably in the case of “weak” grids. The **star-delta-starting** reduces the starting current down to 1/3. Unfortunately, also the starting torque is reduced down to 1/3.

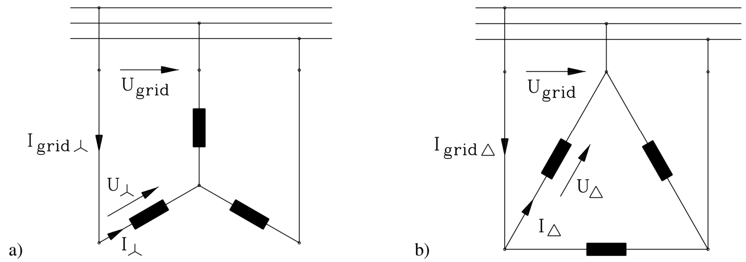

Fig 7.5: Connections of a star-delta-running up: a) star-connection, b) delta-connection

The starting is done in star-connection. Then, it is changed to delta-connection using a special switch (“star-delta-switch”).

Star-connection:
The phase voltage U_Y is $U_{grid}/\sqrt{3}$. The phase current I_Y equals the line current $I_{grid\,Y}$.
Delta-connection:
The phase voltage U_Δ equals the line voltage U_{grid}. The phase current I_Δ is about $1/\sqrt{3}$ smaller than the line-current $I_{grid\Delta} = \sqrt{3} I_\Delta$.

Therefore, the phase voltage at star-connection is by $1/\sqrt{3}$ smaller than at delta-connection:

$$U_Y = \frac{U_\Delta}{\sqrt{3}} \tag{7.16a}$$

The phase current is reduced to the same extent.

$$I_Y = \frac{I_\Delta}{\sqrt{3}} \tag{7.16b}$$

Hence, the line current in Y-connection is only 1/3 of the one at delta-connection:

$$\boxed{I_{gridY} = \frac{I_{grid\Delta}}{\sqrt{3}\cdot\sqrt{3}} = \frac{I_{grid\Delta}}{3}} \tag{7.17}$$

The torque of an induction machine changes with the square of the phase voltage and is therefore also only 1/3 in Y-connection.

$$\boxed{\frac{M_{1Y}}{M_{1\Delta}} = \left(\frac{U_Y}{U_\Delta}\right)^2 = \left(\frac{1}{\sqrt{3}}\right)^2 = \frac{1}{3}} \tag{7.18}$$

<u>*Example 7.2-2:*</u>
Double squirrel cage motors: typical torque M_1 at s = 1: Table 7.1.

	M_1/M_N	I_1/I_N
Δ-connection	2....3	6....8
Y-connection	0.7....1	2 ... 2.7

<u>Table 7.1:</u> Reduction of starting current and starting torque by means of star-delta-connection, values typical for double squirrel cage motors

<u>d2) Soft Starter:</u>
A part of the "voltage-time-area" of the sinusoidal line voltage is "cut" out using anti-parallel thyristors per phase and phase control (Fig. 7.6a). The motor is supplied with a non-sinusoidal voltage. The fundamental of this voltage is reduced when compared with the line-voltage, therefore, the current is reduced, but so is also the generated torque.

<u>d3) Starting Resistors at Slipring-Induction Motors:</u>
Heavy duty starting means that
- the moment of inertia of the load is much larger than the one of the motor or
- the torque of the load is very large.

For such applications, often, line-fed squirrel-cage motors cannot be used, because of thermal reasons (too much heat generation in the rotor). The cage is thermally overstrained: e.g., the bar-ring connection breaks because of uneven thermal expansion. This problem can be avoided by means of inverter-operation (Chapter 7.7) or by use of a slipring-induction motor and **"starting resistors"** in the rotor circuit (Chapter 5). The torque can be kept constant during running up by continuous reduction of the starting resistors (Fig. 7.6b, graph 1). Thereby, running up with breakdown torque to accelerate a heavy load is possible, because the major part of the rotor losses is dissipated in external rotor resistances which can be cooled separately.

In the case of a moderate load torque but a **very weak grid** that cannot cope with the starting current of a squirrel-cage motor, a slipring induction motor may also be used, e.g. for running up with about rated torque and rated current (Fig. 7.6b, graph 2). However, slipring-induction machines are much more expensive than squirrel-cage machines. Therefore, inverter-fed squirrel-cage motors are generally used today for such applications.

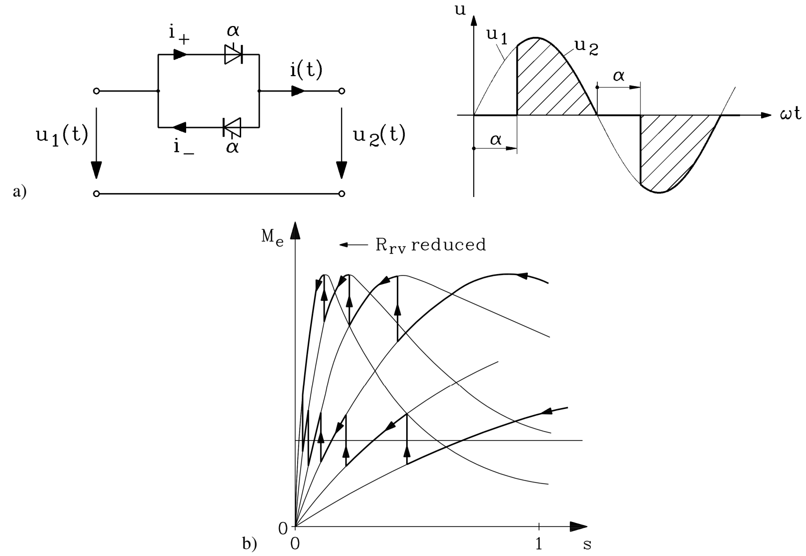

<u>Fig. 7.6:</u> Starting assistances: a) soft starter (power electronics, α: firing angle of thyristors), b) asynchronous running up of a slipring-induction motor with continuously decreasing starting resistor: running up at breakdown torque (upper graph) and rated torque (lower graph)

7.3 Stable and Unstable Working Points – "Quasi-static Stability"

The working point of a motor (n^*, M_e^*) is determined by the point of intersection of the torque-speed characteristic of motor and load ($M_e(n)$ and $M_s(n)$ characteristic) (Fig. 7.7). However, not every point of intersection (working point) is stable.

- Stable Operating Point: In case of small disturbances of speed or torque, the machine returns to the original operating point after the disturbance has faded away.
- Unstable Operating Point: In case of small disturbances of speed or torque, the machine does not return to the original operating point.

The technique of **"quasi-static stability analysis"** uses stationary torque-speed characteristics $M_e(n)$ and $M_s(n)$, which have been linearised in the operating point (**"calculation of small perturbations"**). With the difference of the mechanical speed of rotation due to disturbance Ω_m and the ideal one Ω_m^* of the operating point $\Delta\Omega_m = \Omega_m - \Omega_m^*$ (where $\Omega_m^* = 2\pi n^*$) and the gradient of the characteristics in the operating point

$$\frac{dM_e}{d\Omega_m} = M'_e\,,\ \frac{dM_s}{d\Omega_m} = M'_s$$

the tangents at the characteristics in the operating point are used as linearization:

$$M_e(\Omega_m) \cong M_e(\Omega_m^*) + M'_e \cdot \Delta\Omega_m \tag{7.19a}$$

$$M_s(\Omega_m) \cong M_s(\Omega_m^*) + M'_s \cdot \Delta\Omega_m \tag{7.19b}$$

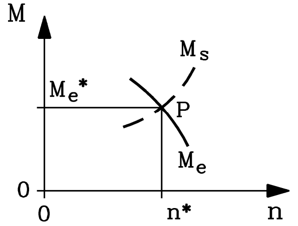

Fig. 7.7: The operating point of the drive (index *) is given by the intersection of the *M(n)* characteristics of motor and load

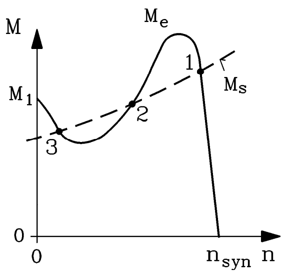

Fig. 7.8: Asynchronous torque characteristic M_e with “saddle” (e.g. double-cage rotor) and torque characteristic M_s of the load: Points 1 and 3 are stable, 2 is unstable.

At the operating point, the torque of motor and load are equal: $M_e(\Omega_m^*) = M_s(\Omega_m^*)$. Using $d\Omega_m / dt = d\Delta\Omega_m / dt$, equation (7.5) becomes:

$$J \cdot \frac{d\Omega_m}{dt} = M_e(\Omega_m) - M_s(\Omega_m) \quad \Rightarrow \quad J \cdot \frac{d\Delta\Omega_m}{dt} - (M'_e - M'_s) \cdot \Delta\Omega_m = 0 \tag{7.20}$$

This is a linear, homogeneous 1st order differential equation for $\Delta\Omega_m$. The solution is the exponential function (7.21).

$$\Delta\Omega_m(t) \sim \exp\left(t \cdot \frac{M'_e - M'_s}{J}\right) \tag{7.21}$$

Result:
If $dM_e / d\Omega_m - dM_s / d\Omega_m > 0$, *the perturbation of the speed (= difference from the speed in the operating point) increases with time; this operating point* ***is unstable****. If the exponent is negative, the perturbation decreases exponentially; the operating point* ***is stable****.*

Example 7.3-1:
Induction motor with “saddle” in the $M_e(n)$ characteristic (Fig. 7.8):
The operating points 1 and 3 are stable, point 2 is unstable (Table 7.2). This motor would stay at point 3 during running up and will not reach point 1.

	operating point	$dM_e/d\Omega_m$	$dM_s/d\Omega_m$	$dM_e/d\Omega_m$ - $dM_s/d\Omega_m$
1	stable	<0	>0	<0
2	unstable	>0	>0	>0
3	stable	<0	>0	<0

Table 7.2: Stability of operating points 1, 2, 3 of Fig. 7.8

7.4 Braking of Induction Machines

a) Mechanical Running Down without Braking:
If the induction machine is separated from the grid, the accelerating torque M_e becomes zero. Only the braking torque M_s of the coupled load and the (very small) braking torque due to friction losses of the induction machine itself M_d remain. The speed of the uncoupled induction machine ($M_s = 0$), where the torque due to losses is supposed to be linear dependent from the speed $M_d = -K_d\Omega_m$, decreases exponentially with the speed as a function of time:

$$J_M \frac{d\Omega_m}{dt} + K_d \cdot \Omega_m = 0 \quad \Rightarrow \quad \Omega_m(t) = \Omega_{m0} \cdot \exp(-\frac{t}{J_M / K_d}) \tag{7.22}$$

The speed of the machine decreases down to $1/e$ within the time constant J_M/K_d. After about 3 time constants, the machine is at stand-still.

Result:
The larger the polar moment of inertia and the smaller the braking frictional torque, the longer takes the running down. With large machines, it may take several hours.

Therefore, special methods are used for **systematic stopping** of drives. Here, the electromagnetic torque M_e itself is used for braking.

b) Braking by Reversal

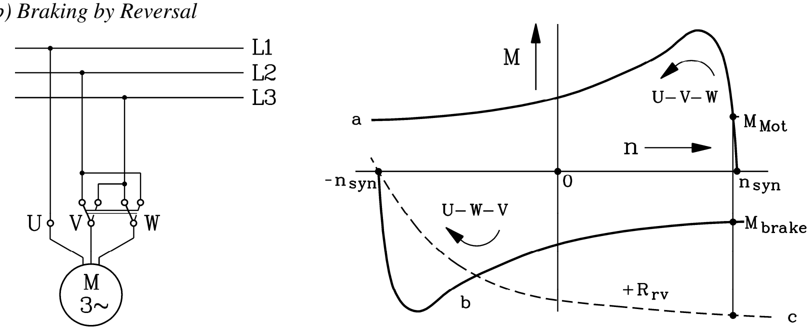

Fig. 7.9: Braking by reversal: If the terminals of two phases are interchanged, the rotating field and the torque change to opposite sign (graph b instead of graph a) and slow the motor down. At $n = 0$, the motor is separated from the supplying grid. In the case of a slipring-induction motor, the braking torque can be maximised by use of external resistances in the rotor circuit (braking torque!, graph c).

By **interchanging the terminals of two phases**, the rotating field that is generated by the stator changes its direction of rotation. The rotor stays with the original direction of rotation because of its moment of inertia J. Therefore, M_e **acts opposite to the direction of rotation** and brakes the rotor down to $n = 0$ (Fig. 7.9). Note, that at $n = 0$, the torque accelerates, so that the motor runs up to negative synchronous speed $-n_{syn}$ against the original direction of rotation. Therefore, it has to be separated from the grid at $n = 0$.

At braking (slip $s > 1$), the induction machine consumes both electric power from the grid via the stator ($P_{in} \sim P_\delta$) and mechanical power P_m via the rotor (kinetic energy from slowing down). Both are converted into heat in the form of losses (Fig. 7.10).

$$P_{Cu,r} = sP_\delta = -(1-s)P_\delta + P_\delta = |P_m| + |M_e\Omega_{syn}| \tag{7.23}$$

Result:
If the stator resistance and all other losses except for $P_{Cu,r}$ are neglected, ***the total consumed power is converted into copper losses in the rotor winding*** *according to (7.23).*

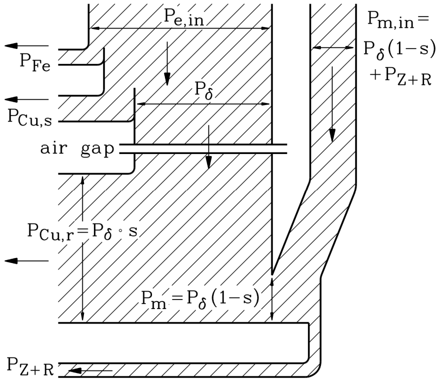

Fig. 7.10: Power flow of an induction machine at braking by reversal of field rotation

c) Generator (Supersynchronous) Braking:
If an induction machine is driven **beyond synchronous speed**, the slip changes to opposite sign ($s < 0$) and so does the sign of the torque, so that the motor brakes (power flow: see Chapter 5). If all losses except for $P_{Cu,r}$ are neglected, the consumed mechanical power is partly converted into heat in the rotor windings, but is – notably at slip with small absolute value – supplied to the grid as electric power ($P_\delta < 0$).

$$P_{Cu,r} = sP_\delta = -(1-s)P_\delta + P_\delta = |P_m| - |P_\delta| = |P_m| - |M_e \Omega_{syn}| > 0\,, \quad P_\delta < 0 \tag{7.24}$$

Generator braking is done e.g. at downhill run of an electric traction vehicle (**"regenerative braking"**).

d) Direct Current Brake:
The machine is separated from the grid. Two of the three phases are supplied with a **direct current** I_d via a dc voltage U_d (Fig. 7.11). The three phase windings generate a static air gap field B with the same number of poles $2p$ as the corresponding three-phase rotating field. The rotor rotates with the original speed n against this field due to its inertia J. Thereby, alternating voltages with the rotor frequency $f_r = n \cdot p$ are induced in the rotor that cause rotor currents I'_r with the same frequency. **Together with the static stator field**, these rotor currents generate a **braking torque** M_e. At $n = 0$, this torque vanishes, because it is $f_r = 0$. No rotor currents are induced any more. According to Fig. 7.11a, the dc-current of the stator I_d can be seen as an instantaneous value of a "frozen" three-phase system (r.m.s.-value $I_s = \sqrt{2/3} \cdot I_d$) at the time when one phase is at zero current. Therefore, the T-equivalent circuit of the induction machine can be used to calculate M_e at a **given current** I_s (Fig. 7.12a). The rotor current I'_r can be derived from the equivalent circuit:

$$\underline{I}'_r = -\underline{I}_s \cdot \frac{jX_h}{\dfrac{R'_r}{s} + jX'_r} \tag{7.25}$$

The braking torque is obtained from the power of the rotating field and the rotor losses:

$$M_e = \frac{P_\delta}{2\pi n_{syn}} = \frac{P_{Cu,r}/s}{2\pi n_{syn}} = \frac{m_s R'_r I'^2_r/s}{2\pi n_{syn}} = \frac{m_s}{2\pi n_{syn}} \cdot \frac{sR'_r X_h^2}{R'^2_r + s^2 X'^2_r} I_s^2 \tag{7.26}$$

Here, the slip is defined according to Chapter 5 as $s = f_r/f_N$, where f_N is the frequency of the grid, and it is $n_{syn} = f_N/p$. The torque characteristic of this "current operated" induction machine is "sharper" (Fig. 7.12b) than the one of the "voltage operated" induction machine as discussed in Chapters 5 and 6, because the breakdown slip s_b is significantly smaller by the factor σ (7.27).

$$dM_e/ds = 0 \quad \Rightarrow \quad s_b = \frac{R'_r}{X'_r} \tag{7.27}$$

For comparison: Breakdown torque in Chapter 5: $s_b = R'_r/(\sigma X'_r)$ for $R_s = 0$! Due to the "sharp" torque characteristic, the braking torque is rather small for a wide speed range, except close to $n = 0$.

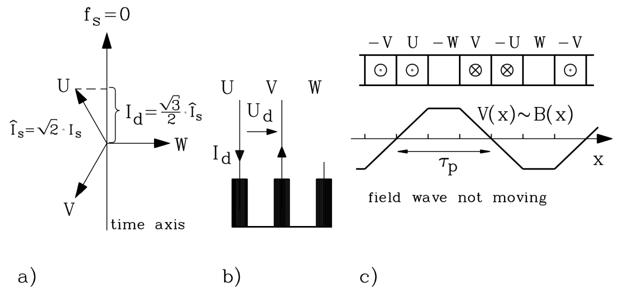

Fig. 7.11: Direct current braking:
a) Direct current as "instantaneous value" of an equivalent three-phase system
b) Electric connection of the stator winding at direct current supply
c) Static air gap field with $2p$ poles excited by direct current (slotting assumed $q \to \infty$)

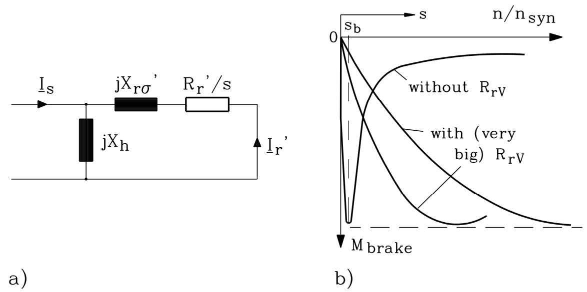

Fig. 7.12: Direct current braking: a) T-equivalent circuit at current I_s
b) Braking torque (without and with external rotor resistances R_v)

Result:
The braking effect of dc braking is relatively small – except in the case of slipring-induction machines. There the breakdown slip can be artificially increased via external rotor resistances ($s_b = (R_r + R_v)/X_r$, Fig. 7.12b).

Remark:
The graph of the braking force as it is shown here is basically identical with the graph of the braking force of an **eddy current brake** that has the same functional principle. In the most simple case, it is a copper disc that rotates between the pole shoes of a dc magnet. It is optimised to give a high braking torque. Such brakes are used in electric test fields to brake the motors under test. A **linear eddy current brake** is also used in the ICE 3, where the rails act as the secondary part.

7.5 Variable Speed Operation of Induction Machines

Variable speed drives are used in fields where variable torque and speed is needed for appropriate operation of the driven load. This is explained in Fig. 7.13 with the example of lifting machines (crane, elevator, ...).

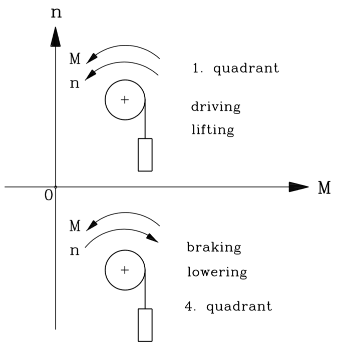

Fig. 7.13: Lifting and lowering of a load requires variable speed operation in both directions of rotation

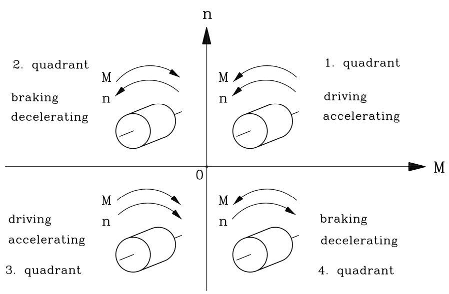

Fig. 7.14: Four-quadrant operation of a variable speed drive

Example 7.5-1:
Elevator drive:
A load shall be lifted from its initial position (e.g. 5th floor) to its final position (e.g. 11th floor). The induction machine has to accelerate against the torque of the load with its torque M up to the requested speed (corresponding to the motor speed n). The acceleration has to be limited to about $0.1g = 1\ \mathrm{m/s^2}$ in the case of people elevators due to reasons of comfort. As the drive arrives its final position, it is stopped by means of a position switch. Speed as well as torque are positive during lifting; the drive operates in the **1st quadrant** of the “*M-n*-plane”; the induction machine operates as a motor (Fig. 7.13).
During lowering of the load, the torque of the load accelerates the drive into the opposite direction ($n < 0$). The torque that is generated by the induction machine M has to brake the load, so that it does "fall down" with uncontrolled high speed. So, electromagnetic torque still acts into positive direction; speed and torque have opposite sign (**4th quadrant**, $n < 0$, $M > 0$), the power is negative. The induction machine operates as a generator brake.

Example 7.5-2:
Drive of an Electric Car:
An electric drive e.g. for an electric car or an electric locomotive must be able to drive and to brake in **both** rotational directions of the machine. Therefore, all four combinations

$n > 0, M > 0$ forward driving
$n > 0, M < 0$ forward braking
$n < 0, M < 0$ backward driving
$n < 0, M > 0$ backward braking
are needed (**four-quadrant operation**, Fig. 7.14).

Induction machines are, because of their small rated slip at line-operation at constant stator frequency, almost **constant speed drives** that operate close to synchronous speed. Operation at variable speed can be obtained as follows:
a) The speed of slipring-induction machines can be changed by use of external **resistances in the rotor circuit**.
b) **Pole-changing stator windings** of squirrel-cage induction machines provide a coarse speed stepping.
c) Operation at variable stator voltage by use of an **ac power controller**, which is shown in Fig. 7.6a: It allows – as it is $M \sim U^2$ – variable speed operation if the requirements are simple. The slip increases significantly at small voltages, so one gets variable speed.
d) Slipring-induction machines can change speed if the rotor is supplied with an additional voltage with rotor frequency (**“doubly-fed induction machine”**).
e) **Frequency inverters** supply a three-phase system of variable frequency and amplitude, thus allowing variation of the motor speed.

a) Slipring-Induction Machine – Speed Variation by External Rotor Resistances:
Fig. 7.15 shows a two-quadrant operation of an elevator (constant load torque M_s) according to Fig. 7.13 with a slipring-induction machine. The speed can be decreased down to zero or even reversed, if **external resistances R_{rv} of increasing number are added to the rotor circuit**. Then, **the terminals of two phases** of the stator winding are **interchanged**; the direction of the field reverses, the induction machine brakes supersynchronously. However, this method to adjust the motor speed has high losses in the rotor (high slip s!) and no more used nowadays.

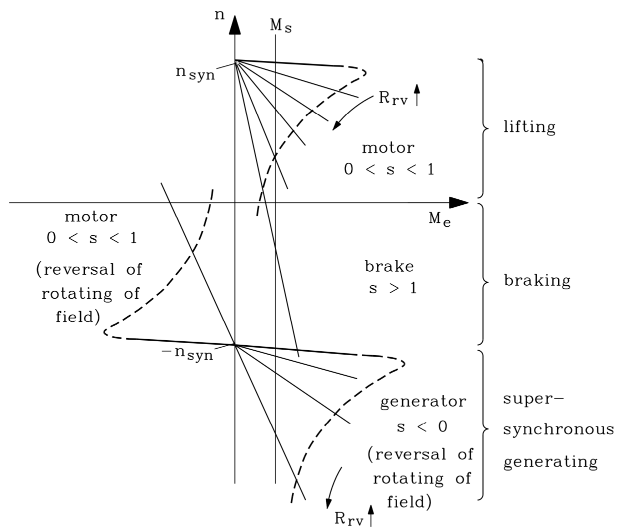

Fig. 7.15: Lifting and lowering of an elevator cabin with use of a slipring-induction machine

b) Pole-changing Induction Machines:
It is possible to arrange **several three-phase windings** with different numbers of poles in the stator slots. Thereby, the machine can be operated with different synchronous speed, using the corresponding winding.

<u>*Example 7.5-3:*</u>
Squirrel-cage induction motor: 48 stator slots:
- two-pole winding, number of slots per pole and phase $q = 8$,
- four-pole winding, number of slots per pole and phase $q = 4$,
- eight-pole winding, number of slots per pole and phase $q = 2$.

Speed levels at 50 Hz: 3000/min, 1500/min, 750/min.
In average, each winding may only use one third of the slot cross sectional area, therefore the thermal power per speed level is only one third of the thermal power of a "single-speed" machine with comparable size.

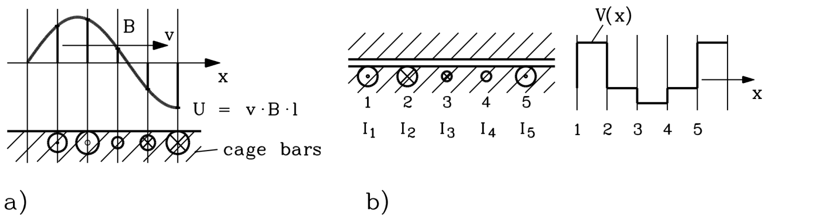

<u>Fig. 7.16:</u> A squirrel-cage (a) can be induced by a rotating field of any number of poles and (b) can also generate a field of any number of poles.

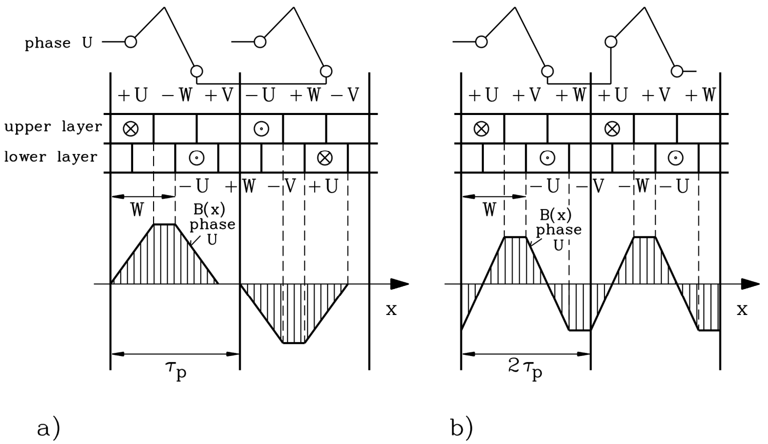

<u>Fig. 7.17:</u> Pole-changing winding according to DAHLANDER (shown: generated field of phase U at infinitively fine slotting ($q \to \infty$)): a) two-pole connection: 6-phase belt winding, short-pitching ½, b) four-pole connection: 3-phase belt winding, fully-pitched

The **squirrel cage adapts to every number of stator poles by itself** (Fig. 7.16). A slipring rotor would need several windings in the stator and in the rotor, so that always the same number of poles could be generated in the stator and in the rotor. The voltage induction of e.g.

a field wave of a two-pole stator field in a four pole rotor winding is zero (why?). No torque would be generated in this case. Therefore, pole-changing slipring-induction machines are not designed.

Special windings exist which allow to generate fields with two different numbers of poles using only ONE winding, depending on the method of connection (*DAHLANDER*-connection $p_1 : p_2 = 1 : 2$ (Fig. 7.17), *KREBS*-connection $p_1 : p_2 = 2 : 3$).

If the winding branches are connected with opposite orientation, the well-known **six phase belt winding with a low number of poles**, e.g. $2p = 2$, is obtained. Upper and lower layer are arranged in a way to give a short-pitch of ½. If the winding branches are connected as series connection with the same orientation of the winding, the **number of poles is doubled** (e.g. $2p = 4$). Each pole pair has only three phase bands (+U, +V, +W) instead of six (+U, -W, +V, -U, +W, -V) (**three phase belt winding**), but the coils are fully-pitched, because the pole pitch is reduced to ½. The terminals of two phases have to be interchanged, to avoid reversal of the rotating field during the change of the number of poles. For each number of poles, the full thermal capacity can be used, because the total stator winding carries the current. The coarse stepping of the speed is often sufficient for fan applications ("big air flow" at high motor speed, "small air flow" at low motor speed, "no air flow" at stand-still).

<u>*Example 7.5-4:*</u>
Pole-changing tunnel fan drive: f_N = 50 Hz: $P_{Lü} \sim n^3$
Four-pole connection: n = 1500/min, $P_{Lü}$ = 800 kW, 100 % air flow
Eight-pole connection: n = 750/min, $P_{Lü}$ = 100 kW, 50 % air flow

c) Doubly-Fed Induction Machine:
If the rotor of a slipring-induction machine is supplied with an **additional voltage** U'_r with slip frequency, this acts – from a simplified point of view - in the same way as the voltage drop at external rotor resistances to obtain variable speed as described above. However, this method allows one additional degree of freedom, which is the phase angle between $\underline{U}'_r$ and the rotor current $\underline{I}'_r$. Thereby, the **synchronous speed can be varied**, although the synchronous speed of the stator field remains constant, **and** the active as well as the reactive current consumed by the machine can be influenced. This is explained using a simplified T-equivalent circuit ($R_s = 0, L_{s\sigma} = 0$) (Fig. 7.18).

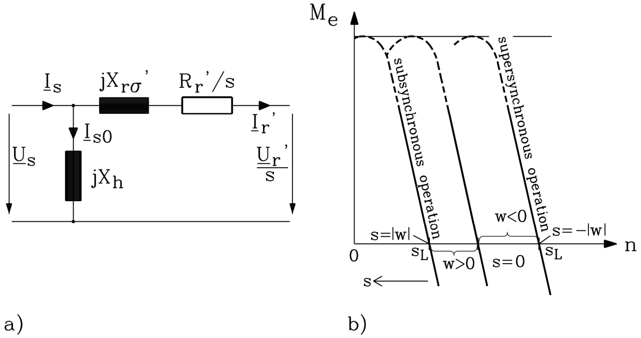

<u>Fig. 7.18:</u> Doubly-fed induction machine:
a) simplified equivalent circuit with additional rotor voltage U'_r,
b) $M_e(n)$ characteristic for different rotor voltages, $w = U'_r/U_s$

The voltage equations for the stator and the rotor circuit of the simplified equivalent circuit Fig. 7.18a

$$\underline{U}_s = jX_h(\underline{I}_s - \underline{I}'_r) = jX_h\underline{I}_{s0} \qquad (7.28)$$

$$\underline{U}'_r = -(R'_r + jsX'_r)\underline{I}'_r + jsX_h\underline{I}_s \qquad (7.29)$$

are solved to give the solutions for $\underline{I}_s, \underline{I}'_r$.

$$\underline{I}_s = \underline{I}_{s0} + \underline{I}'_r \qquad (7.30)$$

$$\underline{I}'_r = \frac{\underline{U}_s - \dfrac{\underline{U}'_r}{s}}{\dfrac{R'_r}{s} + jX'_{r\sigma}} \qquad (7.31)$$

The magnetising current $\underline{I}_m$ equals the no-load current $\underline{I}_{s0}$ here also at load ($\underline{I}'_r \neq 0$), because of the described simplifications, $R_s = 0$, $L_{s\sigma} = 0$.

$$\underline{I}_{s0} = \frac{\underline{U}_s}{jX_h} \qquad (7.32)$$

The amplitude of the additional rotor phase voltage converted to the stator side U'_r can be expressed as a fraction or a multiple of the stator phase voltage. The ratio of the in phase component is w, of the reactive component is b (w: "wirk" – "active", b: "blind" – "reactive").

$$\underline{U}'_r = \underline{U}_s \cdot (w - jb) \qquad (7.33)$$

The electromagnetically generated torque M_e is calculated from the power consumed by the machine P_{in} for the approximation of small slip $s << 1$. The power supplied by the grid P_{in} equals the power of the rotating field P_δ, because it is $R_s = 0$.

$$\underline{I}'_r = \frac{s\underline{U}_s - \underline{U}'_r}{R'_r + jsX'_{r\sigma}} \approx \frac{s\underline{U}_s - \underline{U}'_r}{R'_r} = \frac{\underline{U}_s}{R'_r}(s - w + jb) \text{ for } s << 1 \qquad (7.34)$$

$$P_{in} = m_s \operatorname{Re}\{\underline{U}_s \cdot \underline{I}_s^*\} = m_s \operatorname{Re}\{\underline{U}_s \cdot (\underline{I}_{s0}^* + \underline{I}'^*_r)\} = m_s \operatorname{Re}\{\underline{U}_s \cdot \underline{I}'^*_r\} = m_s \frac{U_s^2}{R'_r}(s - w) = P_\delta \qquad (7.35)$$

$$M_e = \frac{P_\delta}{\Omega_{syn}} = \frac{m_s U_s^2}{\Omega_{syn} R'_r}(s - w) \qquad (7.36)$$

For small slip, the torque characteristic $M_e(s)$ is a straight line (Fig. 7.18b). The breakdown torque and the area of large slip is not described by this approximation. This is not of importance, because the slip of the induction machine is small during steady state operation.

Result:
*The real part of the additional rotor voltage $w = U'_{r,re}/U_s$ causes a **parallel displacement of the M_e-n-characteristics**.*

If the additional rotor voltage is zero ($w = 0$, $b = 0$), the torque – as it is the case with every induction machine with a shorted rotor circuit – vanishes also at $s = 0$. In case of $w \neq 0$, the torque is only zero at slip $s_L = w$. The slip s_L is positive (**SUBsynchronous no-load point**) if the real part of the additional rotor voltage is IN PHASE with the stator voltage; it is negative (**SUPERsynchronous no-load point**) if the PHASE ANGLE between $\underline{U}_s$ and $\underline{U}'_{r,re}$ is 180°.

$$M_e = 0 \quad \Rightarrow \quad s - w = 0 \quad \Rightarrow \quad \boxed{s_L = w = \frac{U'_{r,re}}{U_s}} \qquad (7.37)$$

Result:
The magnitude of the real part of U'_r allows speed variation of doubly-fed induction machines. The imaginary part $\underline{U}'_{r,im} = -jb\underline{U}_s$ allows to vary the consumption of reactive stator current from the grid in order e.g. to obtain a unity or even capacitive power factor.

Applications:
c1) Wind power plants:
In **wind power plants**, doubly-fed induction machine are used as generators if the wind turbine shall not be operated at constant speed. The advantage is that maximum power can be taken out of the wind energy at varying wind speed v. As it is $P_{Wind} \sim v^3$ and $P_{Turbine} \sim n^3$, the power generated by the turbine can be adapted to the wind speed by a variable turbine speed n. The additional rotor voltage with slip frequency can be supplied to the rotor via sliprings by a four-quadrant frequency converter.

Example 7.5-5:
Wind speed fluctuates between $0.65v_{max}$ and v_{max}:
The generator and the gear between turbine and generator are designed to allow for a speed range of $n_{syn} \pm 20\%$ ($s = \pm 0.2$).

Wind speed	Generator speed	Slip	Additional voltage	Power
v_{max}	$n = 1.2n_{syn} = n_{max}$	$s = -0.2$	$w = -0.2$	$P = 100\%$
$v_{min} = 0.65v_{max}$	$n = 0.8n_{syn} = 0.65n_{max}$	$s = +0.2$	$w = +0.2$	$P = 30\%$

Table 7.3: Doubly-fed induction machine as wind generator

The rated power of the converter is given by continuous operation with rated torque at maximum speed

$$P_{converter} = sP_\delta \approx sP_N = 0.2P_N$$

In the example, this is only 20% of the rated power of the machine, which is a cost effective solution. Modern wind power plants for off-shore operation are designed up to 5 MW, 20 /min ±30 % with a wind rotor diameter of 120 m.

c2) Pumped-storage power station:
The energy demand on the grid fluctuates. This fluctuation increases due to the increasing number of installed wind power plants especially in *Germany* and *Denmark*. Excessive electric energy can be used to pump water into reservoirs and store it as potential energy, which can be used to generated electric power in times of peak power demand (e.g. shortly before noon). Synchronous machines, used both as generator (turbine operation) and motor (pump operation), operate at constant speed. So the pump operates at rated power against the constant pressure of the head of the upper storage basin. Hence only with rated power energy can be stored. Doubly-fed induction machines as motor-generators operate at variable speed, e.g. $n/n_N = 0.9 \ldots 1.05$. As pump/turbine power varies with speed $P \sim n^3$, pump and turbine power change significantly even with small changes in speed. Hence it can be stored energy with variable power, e.g. 73% … 115% of P_N. The speed can be adapted via a relatively small and low cost inverter (e.g. $P_{converter}/P_N = 0.9 \ldots 1.05$) that supplies additional voltage to the rotor, to obtain minimum losses at the requested power.

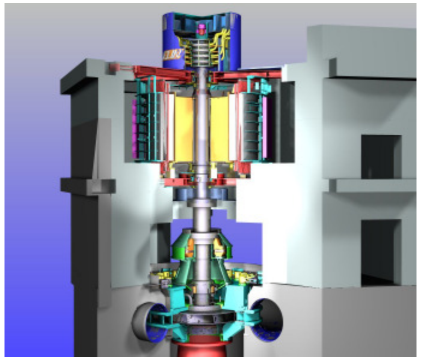

Fig. 7.19: Doubly-fed induction machine as motor-generator with vertical shaft, pumped storage power station *GOLDISTHAL, GERMANY*, P_N = 300 MW, $2p$ = 18, f = 50 Hz, n_{syn} = 333/min, s = ± 10% (300 ... 366/min). Top: sliprings, below: induction machine, bottom: pump-turbine

c2) Rotating Converter Substations for Traction Power Supply:

In some countries (e.g. *Germany, Austria* and *Switzerland*), single-phase series wound motors have been used for long as drive in electric locomotives (Chapter 10), the frequency of the current is 16 2/3 Hz. It is only one third of 50 Hz of the public power supply. Beside power plants with 16 2/3 Hz single-phase synchronous generators that belong to the railway company, supply from the 50 Hz into the 16 2/3 grid is common. It might be suggested, e.g. to couple a six pole 50 Hz three-phase synchronous machine with a two-pole 16 2/3 Hz – single-phase synchronous machine, as both have 1000/min synchronous speed. However, the grid frequencies f_a = 16 2/3 Hz and f_b = 50 Hz cannot be controlled exactly enough to obtain always $f_a = f_b/3$, so the synchronous speed of the two machines always differ slightly. One of both machines would be forced to slip versus the own stator rotating field. No power conversion by a synchronous machine (stator field velocity = rotor field velocity, Chapter 8) would be possible. However, if a six pole doubly-fed 50 Hz-induction machine is used, the $M(n)$-characteristic can be displaced in parallel by means of the additional rotor voltage so that the rated power can be transferred (**rotating converter substations for traction power supply**). The difference in frequency has no longer influence on the power transfer. Since 2003, the German railway grid is operated with 16,7 Hz. Doubly-fed induction machines of rotating converter substations have high power (e.g. 30 MW rated power, converter substation *Ulm, Germany*). The additional rotor voltage is supplied by a frequency converter. Alternatively, the latest converter substations operate ONLY with power electronics, because lower maintenance is needed (e.g. *Jübek, Bremen, Karlsfeld, Germany*).

7. 6 Subsynchronous Converter Cascade

At large power, the inverter on the rotor side for four-quadrant operation is expensive. A special, cheaper solution is the **subsynchronous converter cascade** that contains a simple diode-rectifier. The induced rotor voltage with slip frequency is rectified and then converted to line frequency. Thereby, at **subsynchronous operation** (s > 0), the energy that is usually dissipated as heat in the external rotor resistances $m_r R'_v I'^2_r = sP_\delta - m_r R'_r I'^2_r$ is fed back into the grid. Therefore, a rectifier (at m_r = 3 consisting of six diodes) that is connected to the rotor via sliprings, a smoothing reactor for the rectified rotor current I_d and a line-side converter are

needed. If necessary, the output-voltage of the converter is adapted to the grid voltage via a transformer (Fig. 7.20). The amplitudes $\hat{U}_r$ of the slipfrequent rotor phase voltages $u_{rU}(t), u_{rV}(t), u_{rW}(t)$ decrease proportionally with decreasing rotor frequency $f_r = sf_s$. Hence, they decrease linearly with increasing speed $n = (1-s)n_{syn}$. The rectifier-side dc voltage $u_{dr}(t)$ with a voltage ripple of $6f_r$ and an average value U_{dr} is obtained in the dc-link via a **six pulse rectifier** (Fig. 7.21). U_{dr} has its maximum value U_{dr0} at n = 0 and decreases linear down to zero at synchronous speed (Fig. 7.22). According to Fig. 7.21, the rectified voltage components of the upper and lower 3 rectifying diodes U_{dI} and U_{dII} yield $U_{dr} = U_{dI} + U_{dII} = 2U_{dI}$, where $U_{dI} = 3\sqrt{3}\hat{U}_r/(2\pi)$ and therefore:

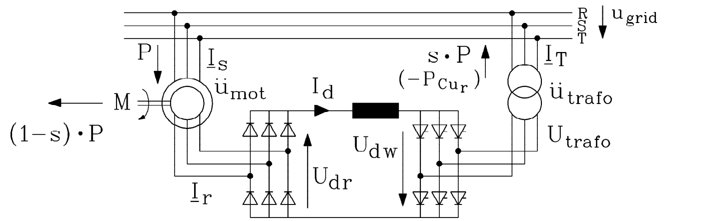

Fig. 7.20: Subsynchronous converter cascade to recover slip energy at variable speed operation $n < n_{syn}$

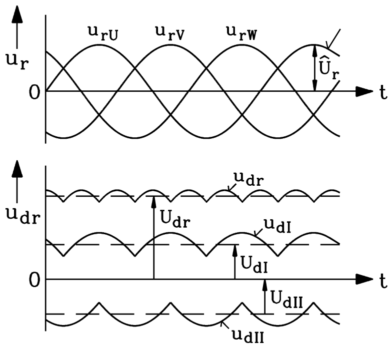

Fig. 7.21: Slipfrequent rotor voltages $u_{rU}(t)$, $u_{rV}(t)$, $u_{rW}(t)$ rectified with a six pulse diode rectifier

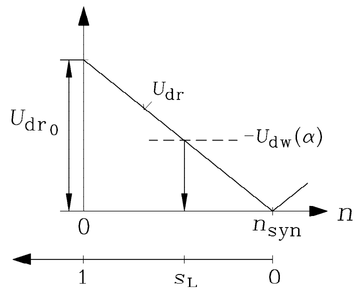

Fig. 7.22: Linear decrease of rectified rotor voltage with increasing speed. The synchronous slip s_L is obtained by variation of the firing angle α of the converter.

$$U_{dr} = U_{dr0} \cdot s \qquad \text{with} \qquad U_{dr0} = U_{dr}(s=1) \tag{7.38a}$$

$$U_{dr} = \frac{3}{\pi}\sqrt{3} \cdot \hat{U}_r \tag{7.38b}$$

The line-side converter rectifies the transformer voltage $u_{trafo}(t)$ with phase voltage amplitude $\hat{U}_{trafo}$ and frequency f_{grid} (Fig. 7.23) as the dc voltage U_{dw}. This voltage U_{dw} can only have a variable average value if it can be influenced by **phase control** with the firing angle α of the firing of the thyristors. So, diodes are sufficient for the rectifier on the rotor side, but not for the line-side converter which needs to be built from thyristors.

$$U_{dw} = \frac{3}{\pi}\sqrt{3}\cdot\hat{U}_{trafo}\cdot\cos\alpha = U_{dw,\max}\cos\alpha \qquad (7.39)$$

Fig. 7.23 shows as an example the phase voltages as they are rectified with a firing angle $\alpha = 90°$. Here, the average value of the rectified voltage is zero: $U_{dw} = 0$. An alternating current I_r (r.m.s.-value) may only flow in the rotor circuit, and a dc current I_d may only flow from the rotor to the grid side in the dc-link, if $U_{dr} > -U_{dw}$. In the reversed case of $U_{dr} < -U_{dw}$, the current flow I_d would reverse, **which is not possible**, because the diodes of the rectifier block such a current flow. Therefore, according to Fig. 7.22, the slip s must be larger than slip s_L, which is determined by (7.39), (7.40), to allow current flow and torque generation. Hence operation is only possible at $s > 0$ as SUBsynchronous speed control.

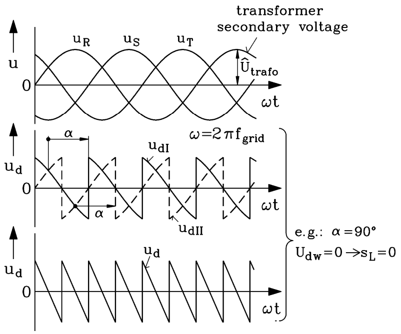

Fig. 7.23: Grid voltage rectified by a converter with firing angle $\alpha = 90°$: The average value of the rectified voltage U_{dw} is zero.

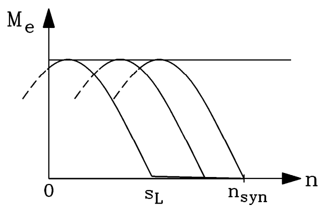

Fig. 7.24: Torque-speed-characteristics of at a **subsynchronous converter cascade** for different firing angles α from 90° to 120°

At **no-load slip s_L**, the rotor is at zero current and it must be $-U_{dw} = U_{dr}$. So the no-load slip is determined and chosen by the firing angle α.

$$U_{dr} = s_L\cdot U_{dr0} = -U_{dw,\max}\cos\alpha \qquad (7.40)$$

Selected Operating Points as Examples:

a) $\alpha = 90°$:

At a firing angle of 90°, it is $s_L = 0$, which corresponds to operation with a shorted rotor, because U_{dw} is zero. The no-load speed of the rotor equals the synchronous speed of the stator rotating field. From $s = 0$ the machine can be loaded, being operated at $s > 0$, which is the $M_e(n)$ characteristic on the right in Fig. 7.24.

b) $\alpha = 120°$:

At $\alpha = 120°$, it is $s_L = 0.5$. The voltage $-U_{dw}$ is always larger than U_{dr} for any slip $0 < s < 0.5$; no rotor current can flow in this region of operation, and no torque can be produced. Only for $s > s_L$, it is $U_{dr} > -U_{dw}$, so that rotor current does flow and torque is generated. The $M_e(n)$ characteristic is shifted to the left in Fig. 7.24).

Rectifier, converter and transformer must be **rated** for rotor power (slip power) at maximum no-load slip s_L, respectively for minimum no-load speed n_L. The slip power is

$P_r = s\cdot P_\delta = \frac{s}{1-s}P_m$. Its maximum value depends on the mechanical power demand $P_m(s)$ of the load. Neglecting rotor losses, the slip power has to be transferred to the grid by the rotor-side power electronics.

Example 7.6-1:

Variable speed water feeder pump for main boiler pump in a 600 MW thermal power plant. Rated power of the pump: $P_N = 12$ MW, rated slip: $s_N = 1$ %, power demand of the pump: $P_m = \left(\frac{n}{n_N}\right)^3\cdot P_N$. Maximum power is delivered at short circuited rotor at $n_N = (1 - s_N)\cdot n_{syn}$.

How big is the rating of the rectifier, the converter and the transformer for an operation range $0.5 \le s_L \le 0$, which means a variation of water flow between 50 % and 100 %?

With the assumption $s_N = 0{,}01 \cong 0$ we get:

$$P_r = \frac{s}{1-s}\left(\frac{n}{n_N}\right)^3\cdot P_N \cong \frac{s}{1-s}\left(\frac{n}{n_{syn}}\right)^3\cdot P_N = \frac{s}{1-s}(1-s)^3 P_N = s(1-s)^2 P_N$$

With $dP_r/ds = 0$ we get the maximum of P_r at $s = 0.33$. Therefore, the rated power for the power electronics is $P_{rN} = P_{r,\max} = 0.33\cdot(1-0.33)^2\cdot 12\,\text{MW} = \underline{\underline{1.78\,\text{MW}}}$, which is only 15 % of the rated machine power.

Result:

The subsynchronous drive is cost effective, notably at high power, because of the low rating of the power electronics, if only a limited speed range is needed (e.g. pump drives).

7.7 Inverter-Fed Induction Machines

a) Voltage Source and Current Source Frequency Inverters:

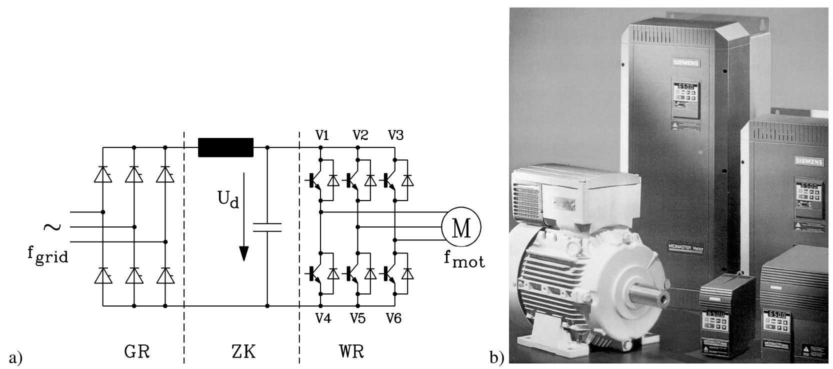

Fig. 7.25: Voltage source inverter: a) power circuit for six step modulation at variable dc-link voltage (GR: "Gleichrichter"-rectifier, ZK: "Zwischenkreis"-dc-link, WR: "Wechselrichter"-converter, V: valve, e.g. switching transistor and free-wheeling diode, M: machine), b) PWM (*P*ulse *W*idth *M*odulation) inverters for power range 0.75 kW up to 75 kW (right); inverter installed inside the motor terminal as "integrated inverter-motor" 7.5 kW (left)

Frequency inverters rectify the three-phase voltages of the line and generate a new three-phase voltage system with variable frequency f_{mot} and voltage amplitude via a converter on the side of the machine. The dc-link between rectifier and converter smoothes the voltage via large dc-link capacitors (**voltage source inverter**, Fig. 7.25) or the current via a large inductance (**current source inverter,** Fig. 7.20). For the machine, a voltage source inverter is a voltage source similar to the feeding grid. Therefore, usage of voltage source inverters is much more common than of current source inverters. Parallel operation of several motors at a voltage source inverter is no problem. Parallel motor operation with a current source inverter is not possible, because of the undefined current sharing at the fixed given dc current operation. The variable output voltage of voltage source inverters can be generated from the dc-link voltage U_d with the converter via **"block modulation (six step modulation)"** or **"pulse width modulation" (PWM)**.

b) Frequency Inverter at Block Modulation:

The power electronic valves V1, V4 (e.g. transistors) respectively V2, V5 and V3, V6 of the converter never must be switched on at the same time, otherwise the dc-link would be shorted! Therefore, each phase can be understood as one switch that switches the corresponding terminal of the machine (phases 1, 2, 3 with the terminals L1, L2, L3) at positive potential $\varphi = U_d/2$ or at negative potential $\varphi = -U_d/2$ (Fig. 7.26a). Thereby, the graphs of the three potentials φ_{L1}, φ_{L2} and φ_{L3} at the motor terminals have the same rectangular shape that changes between $+U_d/2$ and $-U_d/2$, but are displaced by $T/3$ in time (Fig. 7.26b). Here, $T = 1/f_{mot}$ is the new period time determined by the converter. The line-to-line voltage u_{L1-L2} etc. is generating a difference of the potential between the machine terminals L1 – L2 etc.. This mode of operation is called **"block modulation"**, because of the rectangular shape of the voltage graphs with respect to time.

$$u_{L1-L2}(t) = \varphi_{L1}(t) - \varphi_{L2}(t) \tag{7.41}$$

The amplitude of $u_{L1-L2}(t)$ is U_d. This rectangular shaped ac voltage with motor frequency f_{mot} feeds the motor. The dc-link voltage U_d is changed via phase control of the line-side rectifier GR by changing the firing angle α_{GR} in the same way as in (7.39), (see Fig. 7.25a).

Maximum value of the rectified line voltage is obtained at $\alpha_{GR} = 0$: $U_{d,\max} = \frac{3}{\pi}\sqrt{3}\cdot\hat{U}_{grid}$.

The phase voltage u_S of the inverter output at the electric machine's terminals is determined from the mesh equations (Fig. 7.27a).

$$u_{S1}(t) - u_{S2}(t) = u_{L1-L2}(t) \tag{7.42a}$$
$$u_{S2}(t) - u_{S3}(t) = u_{L2-L3}(t) \tag{7.42b}$$
$$u_{S1}(t) + u_{S2}(t) + u_{S3}(t) = 0 \tag{7.42c}$$

By solving (7.42), we derive e.g. for phase 1

$$u_{S1}(t) = \frac{2u_{L1-L2}(t) + u_{L2-L3}(t)}{3}, \tag{7.43}$$

which corresponds to a step like phase voltage variation in time with amplitude $2U_d/3$ (Fig. 7.27b).

The block shaped line-to-line voltage can be expressed as a *FOURIER*-series of time (7.44).

$$\boxed{u_L(t) = \sum_{k=1,-5,7,..}^{\infty}\hat{U}_{L,k}\cdot\cos(k\cdot\omega_s t) = \sum_{k=1,-5,7,..}^{\infty}\frac{2}{\pi}\sqrt{3}\frac{U_d}{k}\cdot\cos(k\cdot\omega_s t)} \tag{7.44}$$

$$\boxed{k = 1 + 6g} \qquad g = 0, \pm 1, \pm 2, ... \qquad \Rightarrow \quad k = 1,\ -5,\ 7,\ -11,\ 13,\ ... \tag{7.45}$$

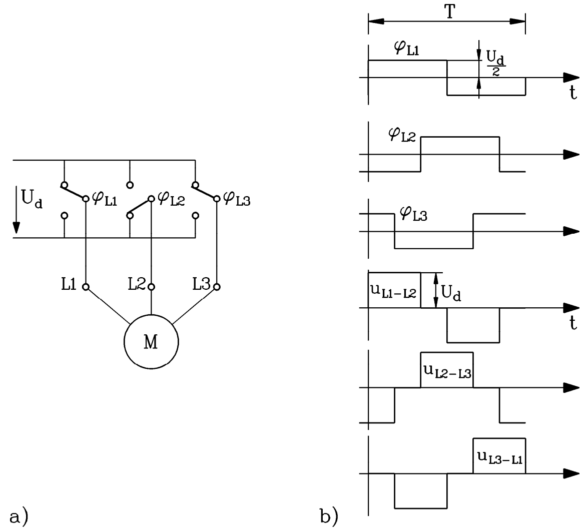

Fig. 7.26: Block modulation of a voltage source inverter:
a) principal sketch of the switching, b) electric potential at the terminals φ and line-to-line voltage u_L

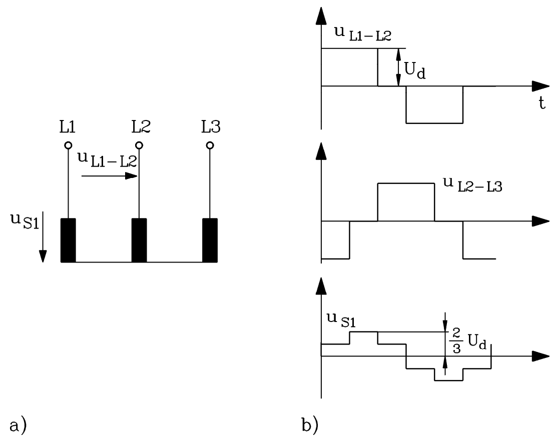

Fig. 7.27: Block modulation (six step modulation) at star-connection of the motor winding: a) phase voltage u_S and line-to-line voltage u_L, b) time characteristic of the line-to-line voltage u_L and the phase voltage u_S

Only odd ordinal numbers k that are not multiples of 3 exist. Please do not confuse these ordinal numbers k with the ordinal numbers ν of the *FOURIER*-series of space of the field waves of Chapter 3! As (7.44) is an alternating series of positive and negative addends, k is defined with a positive or negative sign (7.45).

Result:
The machine receives a blend of sinusoidal voltages with different frequencies of which only the fundamental with k = 1 is desired. The frequency of the fundamental of the voltage $f_{mot} = 1/T = f_s$ *equals the stator frequency of the machine. The harmonics* $|k| > 1$ *cause additional undesired harmonic currents with higher frequency* $|k| f_s$ *in the winding that cause additional losses.*

Example 7.7-1:
Amplitude spectrum of the six-step modulation line-to-line voltage:

k	1	-5	7	-11	13
$\hat{U}_{Lk} / \hat{U}_{L1}$	1	-0.2	0.14	-0.1	0.08

Table 7.4: Amplitudes of the line-to-line inverter-output voltage at block (six step) modulation

c) Performance of Induction Machines at Variable Stator Frequency and $R_s = 0$*:*
As the dominating fundamental of the phase voltage U_s (rms)

$$U_{s,k=1} = \frac{U_{L,k=1}}{\sqrt{3}} = \frac{\sqrt{2}}{\pi} \cdot U_d$$

feeds the induction machine, the fundamental of the current I_s flows in the machine winding. The influence of the harmonics $|k| > 1$ is neglected. As the stator angular frequency ω_s is variable, the reactances X are replaced by the **inductances** $\omega_s L$. The slip s is also expressed by **frequency**.

$$s = \frac{n_{syn} - n}{n_{syn}} = \frac{f_s / p - n}{f_s / p} = \frac{f_s - n \cdot p}{f_s} = \frac{f_r}{f_s} = \frac{\omega_r}{\omega_s} \tag{7.46}$$

The voltage equations of the equivalent circuit – using the simplification $R_s = 0$ – are:

$$\underline{U}_s = j\omega_s L_{s\sigma} \underline{I}_s + j\omega_s L_h (\underline{I}_s + \underline{I}'_r) \tag{7.47}$$

$$0 = (\frac{R'_r}{\omega_r / \omega_s} + j\omega_s L'_{r\sigma}) \underline{I}'_r + j\omega_s L_h (\underline{I}_s + \underline{I}'_r) \tag{7.48}$$

The voltage equations divided by the stator angular frequency ω_s are similar to those of a line-fed machines: There, X occurs instead of L, the slip s instead of the rotor angular frequency ω_r, and the r.m.s.-value of the stator phase voltage instead of the r.m.s. fundamental of the inverter-output voltage divided by ω_s.

$$\frac{\underline{U}_s}{\omega_s} = jL_{s\sigma} \underline{I}_s + jL_h (\underline{I}_s + \underline{I}'_r) \tag{7.49}$$

$$0 = (\frac{R'_r}{\omega_r} + jL'_{r\sigma}) \underline{I}'_r + jL_h (\underline{I}_s + \underline{I}'_r) \tag{7.50}$$

So, at variable rotor frequency ω_r and a with constant value $\underline{U}_s/\omega_s$, the **locus diagram of the stator current phasor** $\underline{I}_s$ **is again a circle**, the circle centre is on the negative imaginary axis because it is $R_s = 0$ (***HEYLAND*'s circle**). This circle is scaled in ω_r instead of s (Fig. 7.28). The "torque line" and "power line" of the circle diagram (Chapter 5) can be also used here. Physically, $\underline{U}_s/\omega_s$ means that the circle diameter and hence the current consumption remain constant, if the amplitude AND the frequency of the voltage are changed **at the same time**.

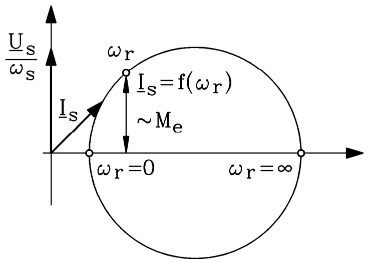

Fig. 7.28: If $\underline{U}_s/\omega_s$ is kept constant and the stator is supplied with variable frequency, the locus diagram of the stator current is a circle that is scaled in ω_r.

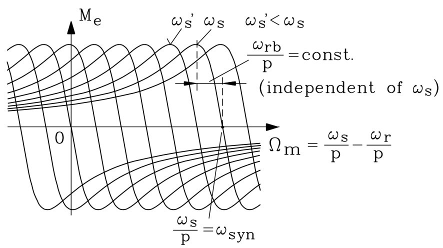

Fig. 7.29: Torque-speed characteristic of an induction machine for different stator angular frequencies ω_s at U_s/ω_s = const. ($R_s = 0$)

$$R_s = 0: \quad \frac{\underline{U}_s}{\omega_s} \cdot \sqrt{2} = j\underline{\Psi}_s = const. \quad \Leftrightarrow \quad \underline{\Psi}_s / \sqrt{2} = L_{s\sigma} \underline{I}_s + L_h (\underline{I}_s + \underline{I}'_r) = const. \tag{7.51}$$

From (7.51), it is derived that the flux linkage of the stator and hence the air gap magnetic field remain unchanged if $\underline{U}_s/\omega_s$ is kept constant. The torque-speed characteristic at variable speed but $\underline{U}_s/\omega_s$ = const. can be obtained via the rotor frequency from the circle diagram (Fig. 7.29). **The same graph** $M_e(\omega_r)$ is obtained for each stator angular frequency ω_s and the corresponding voltage $U_s \sim \omega_s$. If the graphs are drawn as functions

$M_e(n) = M_e(\Omega_m)$,

the shape is always the same, but the graphs are **shifted in parallel** as a function of the stator frequency (Fig. 7.29).

$$\Omega_m = \frac{\omega_s}{p} - \frac{\omega_r}{p} \tag{7.52}$$

It is obvious from the formulas for the torque and the breakdown slip that the torque-speed characteristic at variable ω_s and U_s/ω_s = const. ($R_s = 0$) does only change its position, but not its shape. At $R_s = 0$, according to *KLOSS*'s equation in Chapter 5, the breakdown torque M_b is:

$$M_b = \frac{m_s U_s^2}{\omega_s / p} \cdot \frac{1}{X_s} \cdot \frac{1-\sigma}{2\sigma} = \frac{m_s p}{2} \cdot \left(\frac{U_s}{\omega_s}\right)^2 \cdot \frac{1-\sigma}{\sigma L_s} \qquad (7.53)$$

Due to U_s/ω_s = const., the breakdown torque is constant, independently of the chosen stator frequency ω_s. This is also true for the rotor breakdown frequency ω_{rb} that corresponds to the breakdown slip s_b.

$$s_b = \frac{R'_r}{\sigma X'_r} = \frac{R'_r}{\sigma \cdot \omega_s L'_r} = \frac{\omega_{rb}}{\omega_s} \quad \Rightarrow \quad \omega_{rb} = \frac{R'_r}{\sigma L'_r} = const. \qquad (7.54)$$

If the maximum possible inverter output voltage $U_{s,max} = \sqrt{2}/\pi \cdot U_{d,max}$ is reached, the "rule" U_s/ω_s = const. cannot be respected any longer as ω_s increases further. A further increase of the stator frequency according to (7.55) results in a decrease of the stator flux (**flux weakening region**). The flux and the flux linkage decrease already at no-load hyperbolically with increasing stator frequency. Note, that the corresponding breakdown torque decreases with the reciprocal value of the **square** of the frequency.

$$R_s = 0: \quad \Psi_s = \frac{U_{s,max}}{\omega_s}, \qquad M_b \sim \frac{U_{s,max}^2}{\omega_s^2} \qquad (7.55)$$

The rotor breakdown frequency ω_{rb} remains however constant. Therefore, the gradient dM_e/ds of the $M_e(n)$-characteristic decreases hyperbolically with increasing stator frequency in the flux weakening range, as can be shown by a short calculation using *KLOSS*'s formula.

$$M_e(s) = M_b \cdot \frac{2 \cdot s \cdot s_b}{s^2 + s_b^2} \approx M_b \cdot \frac{2s}{s_b} \quad \text{for} \quad s = \frac{\omega_r}{\omega_s} << 1 \quad \Rightarrow$$

$$\frac{dM_e}{ds} = \frac{2M_b}{s_b} = \frac{2M_b}{\omega_{rb}} \cdot \omega_s \sim \frac{1}{\omega_s} \qquad (7.56)$$

The decrease of the breakdown torque and of the gradient $n(M_e)$ are obvious in Fig. 7.30 that shows $n(M_e)$.

d) Performance of Induction Machines at Variable Stator Frequency and $R_s \neq 0$:

At small angular stator frequency ω_s, the voltage drop at the stator resistance in the stator voltage equation **is no longer negligible** (Example 7.7-2).

$$\underline{U}_s = R_s \underline{I}_s + j\omega_s L_{s\sigma} \underline{I}_s + j\omega_s L_h (\underline{I}_s + \underline{I}'_r) \qquad (7.57)$$

Example 7.7-2:

Typical standard motor with rated parameters f_{sN} = 50 Hz, U_{sN} = 230 V:

a) The following voltage drops at rated frequency and rated current I_{sN} are given:

$$f_s = 50 Hz: \frac{R_s I_{sN}}{U_{sN}} = 6\%, \quad \frac{X_s I_{sN}}{U_{sN}} = \frac{\omega_s L_s I_{sN}}{U_{sN}} = 300\% \quad \Rightarrow \quad \frac{R_s}{\omega_s L_s} = \frac{6}{300} = \underline{\underline{0.02}}$$

The voltage drop at the stator resistance is only 2 % and can be neglected.

b) However, if the motor is operated at **small stator frequency** 5 Hz, the voltage drop at the resistance with respect to the induced stator voltage is 10 times larger than in the case of 50 Hz-supply. The value of the ratio 20% is **no longer** negligible.

$$f_s = 5\,Hz: \frac{R_s}{\omega_s L_s} = \frac{6}{\frac{5}{50} \cdot 300} = \underline{\underline{0.2}}$$

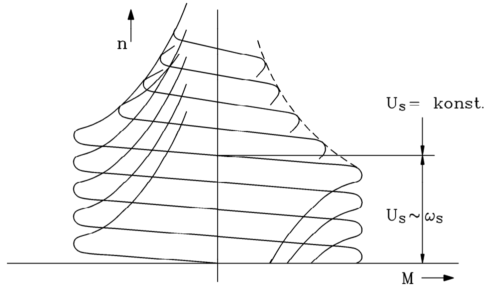

Fig. 7.30: **Torque-speed characteristic** of an inverter-fed induction machine for different stator angular frequencies ω_s at (a) U_s/ω_s = const. (R_s = 0) and (b) in the flux weakening range where U_s = const.

For a given stator phase voltage U_s, the voltage drop at the stator resistance reduces the internal voltage U_h, hence the breakdown torque is reduced with the square $M_b \sim U_h^2$. The stator resistance (Chapter 5) causes the centre of the locus diagram $\underline{I}_s(\omega_r)$ to lie above the abscissa and the circle diameter to decrease. This effect is notably of influence at small frequencies. The smaller diameter of the circle corresponds to the smaller breakdown torque. If the breakdown torque shall remain constant also in the case of small frequencies – as it is the case with R_s = 0 – the circle diameter must be kept constant via an increase of U_s. At R_s = 0, the circle diameter is given by $\underline{I}_s(\omega_r \to \infty) - \underline{I}_s(\omega_r = 0) = \underline{I}_{s\infty} - \underline{I}_{s0}$. As the absolute value of $\underline{I}_{s\infty}$ is significantly larger than the one of $\underline{I}_{s0}$, the absolute value of $\underline{I}_{s\infty}$ can be taken roughly as the circle diameter. It must be constant to obtain a constant circle diameter at small stator frequencies.

$$\underline{I}_{s\infty} = \underline{I}_s(\omega_r \to \infty) = \frac{U_s}{R_s + j\sigma\omega_s L_s} = \text{const.} \qquad (7.58)$$

The **voltage increase** of U_s at small frequencies must meet the following condition (Fig. 7.31):

$$I_{s\infty} = const. \quad \Rightarrow \quad U_s \sim \sqrt{R_s^2 + (\sigma\omega_s L_s)^2} \qquad (7.59)$$

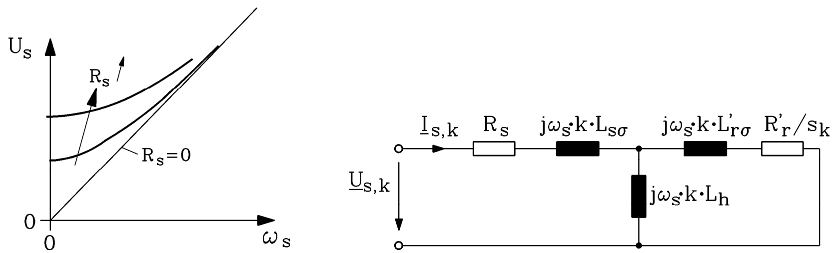

Fig. 7.31: $U_s(\omega_s)$ at small frequencies: Voltage must be increased to compensate the voltage drop at the stator resistance.

Fig. 7.32: T-equivalent circuit of an induction machine for the k^{th} voltage harmonic $U_{s,k}$ of a non-sinusoidal, but periodic stator voltage supply

e) Effects of Current Harmonics:

So far, only the effect of the fundamental of the inverter output voltage on the induction machine has been considered. However, the harmonics of the stator voltage $U_{s,k}$ that feed the machine with k times fundamental frequency kf_s, cause additional flow of harmonic currents $I_{s,k}$ in the stator winding. These currents generate themselves – like the fundamental current I_s – a magnetic field in the air gap with $2p$ poles as a rotating space fundamental wave. Each of these fundamental waves rotates with its own synchronous speed $n_{syn,k}$.

$$n_{syn,k} = k \cdot \frac{f_s}{p} = \frac{1}{2\pi} \cdot k \cdot \frac{\omega_s}{p} \tag{7.60}$$

With the rotor running at speed n, the **harmonic slip** s_k of the rotor with respect to these additional fundamental waves is

$$s_k = \frac{n_{syn,k} - n}{n_{syn,k}} = \frac{kn_{syn} - n}{kn_{syn}} = 1 - \frac{1}{k} \cdot \frac{n}{n_{syn}} = 1 - \frac{1}{k} \cdot (1-s). \tag{7.61}$$

Therefore, the rotor is induced with additional rotor frequencies $s_k \cdot kf_s$ resulting in parasitic harmonic currents $I'_{r,k}$. For each three-phase voltage system of the k^{th} harmonic, a T-equivalent circuit can be given (Fig. 7.32). As it is $|k| >> 1$, the value of the slip s_k is almost 1 for $0 < s < 1$; hence, the rotor seems to be at stand-still when seen from the perspective of the fast travelling rotating waves of the harmonic currents. The amplitude of the k^{th} harmonic $I_{s,k}$ can be estimated from Fig. 7.32, because it is $L_h >> L_{\sigma s}, L'_{\sigma r}$ and $s_k \approx 1$.

$$I_{s,k} \approx \frac{U_{s,k}}{\sqrt{(R_s + R'_r)^2 + (k\omega_s)^2 \cdot (L_{s\sigma} + L'_{r\sigma})^2}} \approx \frac{U_{s,k}}{|k|\omega_s (L_{s\sigma} + L'_{r\sigma})} \tag{7.62}$$

Result:

The harmonic currents $I_{s,k}$ occur nearly independent of the load of the machine (= independent of s) with almost constant magnitude. Hence, they already have full magnitude at no-load $s = 0$.

The value of the frequency of the rotor harmonic currents is – because of $s_k \approx 1$ – nearly $|k| f_s$, which is a very high value. This results in strong current displacement in the massive bars of the squirrel-cage rotor. The current displacement factor $k_R(|k| f_s)$ is large, which results in additional **rotor losses**. A high leakage inductance $L_{s\sigma} + L'_{r\sigma} \cong \sigma L_s$ limits the amplitudes of these currents according to (7.62), but it also reduces the breakdown torque, which is not wanted (7.53). Furthermore, the fast travelling rotating waves of the harmonic currents generate additional torque components together with the rotating wave of the fundamental current. The average of these torque components in time is zero, because of the different travelling speed of the field waves. They occur as **pulsating torque components** and may cause **torsional oscillation** of the shaft of the induction machine and the load (This topic is discussed in detail in the lecture *"Motor Development for Electric Drive Systems"*.)

Example 7.7-3:

Amplitudes of the current harmonics at voltage six-step modulation:

$$I_{s,k} \approx \frac{U_{s,k}}{|k|\omega_s (L_{s\sigma} + L'_{r\sigma})} \sim \frac{1}{|k|^2}$$

k	1	-5	7	-11	13
$\left\| \hat{U}_{Lk} / \hat{U}_{L1} \right\|$	1	0.2	0.14	0.1	0.08
$I_{s,k} / I_{s,k=1}$	1	0.04	0.02	0.008	0.006

Table 7.5: Amplitudes of the stator current harmonics at six-step modulation, with respect to the short-circuit current $I_{s,k=1}$ (s = 1).

Result:

With increasing ordinal numbers the current harmonics decrease much faster than the voltage harmonics, because the leakage inductance "smoothes" the current (Fig. 7.33).

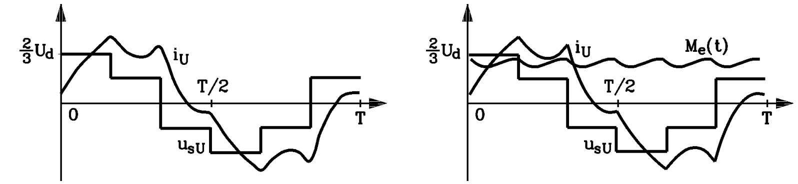

a) b)

Fig. 7.33: Phase current i_U at six-step modulation, calculated as a) *Fourier* sum, b) closed solution with space vectors (see: Lecture "CAD and System Dynamics of Electrical Machines"), showing torque ripple

f) Pulse Width Modulation (PWM):

A fundamental voltage with variable amplitude and frequency can also be generated by **pulse width modulation** (PWM) of the inverter output voltage, WITHOUT the need of an adjustable dc-link voltage U_d. Furthermore, the amplitudes $U_{s,k}$ – notably for low ordinal numbers k – can be significantly reduced. An uncontrolled diode rectifier generates a constant voltage U_d (Fig. 7.34). The on and off commands of the six turn-off power elements of the converter (WR) are obtained by comparison of a saw-tooth signal u_{st} with **switching frequency** f_{switch} and a sinusoidal reference signal u_{ref} that pulsates with the desired stator frequency f_s and has variable amplitude $0 < A_1 < 1$ (**sinusoidal modulation**). At $u_{ref} > u_{st}$, the terminal L1 of the machine is always connected to the positive potential $\varphi = U_d/2$, at $u_{ref} < u_{st}$ it is connected to the negative potential $\varphi = -U_d/2$. Thereby, the potential φ_{L1} at the terminal L1 as function of time pulsates between $+U_d/2$ and $-U_d/2$. In Fig. 7.35a, the amplitude $A_1 = 0.5$ and the ratio $f_{switch}/f_s = 9$ were chosen. The same procedure is applied to the terminals L2, L3, but with $T_s/3$, respectively $2T_s/3$ phase difference ($T_s = 1/f_s$).

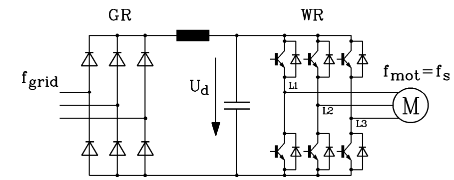

Fig. 7.34: Basic set-up of a PWM voltage source inverter with dc link capacitor and filter choke

The voltage between two terminals, e.g. L1 and L2 is obtained from the difference of the potential of the two terminals according to Fig. 7.34b:

$$u_{L2-L1} = \varphi_{L2} - \varphi_{L1} \tag{7.63}$$

The “pulsed line-to-line voltage” contains pulses with different width but with **twice the switching frequency** $f_p = 2\,f_{switch}$ (**pulse frequency**). The *FOURIER*-analysis of the potential $\varphi_{L1}(t)$ and the voltage $u_{L1\text{-}L2}(t)$ of Fig. 7.35 gives the amplitudes shown in Table 7.6. Due to the symmetry of the signals to the abscissa, only voltage harmonics with odd ordinal numbers k occur.

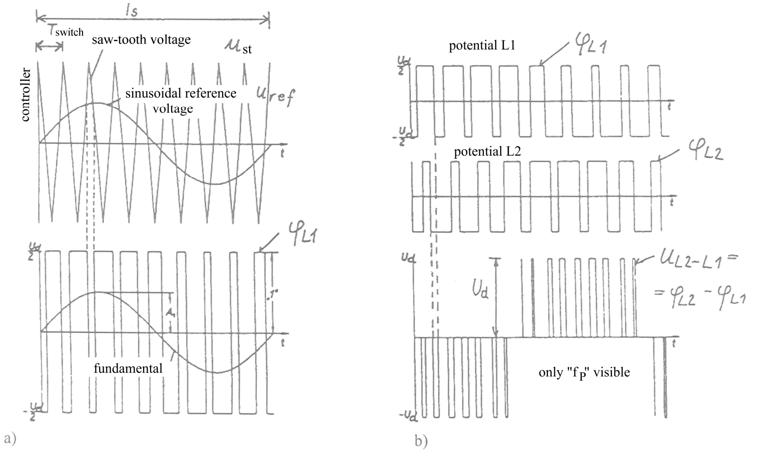

Fig. 7.35: Generation of a pulsed inverter-output voltage using sinusoidal modulation:
a) generation of the potentials $\varphi_{L1}(t)$ at the terminal L1, b) generation of the terminal voltage $u_{L1\text{-}L2}(t)$

$$\varphi_{L1}(t) = \sum_k \hat{\varphi}_k \cdot \cos(k \cdot \omega_s t) \tag{7.64}$$

$$u_{L1-L2}(t) = \sum_k \hat{U}_{L,k} \cdot \cos(k \cdot \omega_s t) \tag{7.65}$$

$\lvert k \rvert$	1	3	5	7	9	11	13	15	17	19
$\hat{\varphi}_k / (U_d/2)$	0.5	$<10^{-5}$	0.001	0.09	1.08	0.09	0.002	0.04	0.36	0.36
$\hat{U}_{L,k} / \hat{U}_{L,k=1}$	1	0	0.002	0.18	0	0.18	0.004	0	0.72	0.72

Table 7.6: Harmonic analysis of the potential $\varphi_{L1}(t)$ and the line-to-line voltage $u_{L1\text{-}L2}(t)$ at inverter operation for $A_1 = 0.5$ and $f_{switch}/f_s = 9$

Result:

The potential at the terminals φ_L contains – beside the fundamental – high amplitudes with switching frequency (k = 9) and about twice the switching frequency (k_p = 17 and 19).

$$k_p = \left| \frac{f_p}{f_s} \pm 1 \right| \qquad \Rightarrow \qquad k_p = |18 \pm 1| = 17, 19$$

As the harmonics with small ordinal numbers that are multiples of 3 do not occur in the line-to-line voltage, the amplitude with switching frequency (k = 9) disappears. The line-to-line voltage – hence, also the current – contains only harmonics with about twice the switching frequency (pulse frequency, Fig. 7.36).

The amplitude of the harmonic with the low ordinal number 5 is very small. The amplitude of the fundamental of the voltage is adjusted via the **“modulation ratio”** (= amplitude A_1 of the reference sinus).

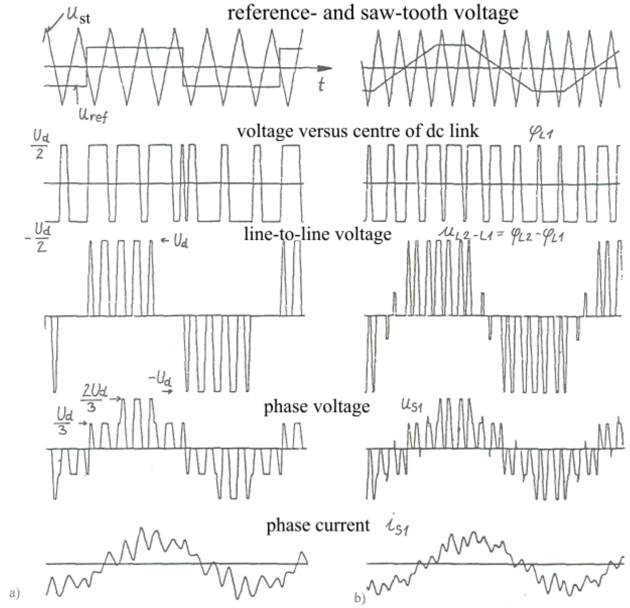

Fig. 7.36: Voltage pattern and current waveform at PWM-inverter operation: a) $f_{switch}/f_s = 6$, rectangular modulation b) $f_{switch}/f_s = 9$, trapezoidal modulation.

Example 7.7-4:
Comparison of different switching frequencies (Fig. 7.36):
With increasing ratio f_{switch}/f_s (Fig. 7.36b !), the current becomes **closer to the ideal sinusoidal waveform**.

The reference voltage u_{ref} must not necessarily be sinusoidal. Rectangular or trapezoidal shape are also possible (Fig. 7.36 a) respectively b)). Nowadays most often space vector modulation is used (see lecture *“Power Electronics”*). In Fig. 7.35 and 7.36 the ratio f_{switch}/f_s is integer, by synchronising reference and saw-tooth voltage ("synchronous modulation"). In many applications, the switching frequency f_{switch} is kept fixed, independent of f_s ("asynchronous modulation").

Example 7.7-5:
Pulse width modulation with fast switching Insulated Gate Bipolar Transistors (IGBT):
f_{switch} = 3 kHz, f_s = 100 Hz: $f_{switch} / f_s = 30$, $f_p = 2f_{switch}$ = 6 kHz: Noticeable voltage and current harmonics occur at the ordinal numbers $k = \left| \frac{f_p}{f_s} \pm 1 \right| = |60 \pm 1| = 59, 61$, respectively at the frequencies $59 \cdot 100 = 5900\,\mathrm{Hz}$ and $61 \cdot 100 = 6100\,\mathrm{Hz}$.